Modeling of in situ ultrafine atmospheric particle formation in the eastern United States

Timothy M. Gaydos and Charles O. Stanier
Department of Chemical Engineering, Carnegie Mellon University, Pittsburgh, Pennsylvania, USA

Spyros N. Pandis
Departments of Chemical Engineering and Engineering and Public Policy, Carnegie Mellon University, Pittsburgh, Pennsylvania, USA

[1]   The creation of new atmospheric particles from in situ nucleation influences climate through cloud-aerosol interactions and may negatively impact human health. Although recent observations show that nucleation is widespread in the eastern United States, the corresponding pathways remain uncertain. Combining extensive field measurements in Pittsburgh, Pennsylvania, with an aerosol dynamics and chemistry model assuming ternary NH_3-H_2SO_4-H_2O nuclei formation, we show excellent model-measurement agreement and predictive capability. The ternary NH_3-H_2SO_4-H_2O nucleation model is successful in predicting the presence or lack of nucleation on 19 out of 19 days with complete data sets in July 2001 and on 25 out of 29 days in January 2002. Reductions of ammonia emissions are predicted to decrease the frequency of nucleation events during both summer and winter, with a more dramatic effect during the summer. The response to changes in emissions of sulfur dioxide during the summer is counterintuitive. Reductions of sulfur dioxide and the resulting sulfate by up to 40% actually increase the frequency of the summer nucleation events. Modeling predicts the opposite effect in winter, with reductions of sulfur dioxide leading to fewer nucleation events.

Citation: Gaydos, T. M., C. O. Stanier, and S. N. Pandis (2005), Modeling of in situ ultrafine atmospheric particle formation in the eastern United States, *J. Geophys. Res.*, *110*, D07S12, doi:10.1029/2004JD004683.

1.   Introduction

[2]   The two major processes introducing new particles into the atmosphere are in situ nucleation and direct emission from sources such as combustion, sea spray, dust, etc. A variety of field measurements show that in situ nucleation occurs in many places around the globe [*Weber et al.*, 1999; *Kulmala et al.*, 2001a; *O'Dowd et al.*, 2002], including urban areas [*Woo et al.*, 2001] where it was previously thought particularly unlikely due to high concentrations of aerosol surface area, which suppress nucleation. These events alter the number and chemical composition of ultrafine particles and cloud condensation nuclei, with implications for human health [*Oberdorster et al.*, 1992; *Ibald-Mulli et al.*, 2002; *Li et al.*, 1999; *Nemmar et al.*, 2002; *Peters et al.*, 1997; *Oberdorster et al.*, 2002] and climate [*Adams and Seinfeld*, 2003]. For example, recent studies comparing the health effects of differently sized particles show that ultrafine (<100 nm) atmospheric particles can have negative health effects, possibly due to their high surface area. Climate can be affected as these particles grow to larger than 100 nm in size.

[3]   Several mechanisms have been proposed for the production of new atmospheric particles including sulfuric acid-water binary nucleation [*Nilsson and Kulmala*, 1998], sulfuric acid-ammonia-water ternary nucleation [*Coffman and Hegg*, 1995; *Weber et al.*, 1998; *Kulmala et al.*, 2002], nucleation of organic vapors [*Hoffman et al.*, 1997], ion-induced nucleation [*Laakso et al.*, 2002], and halogen-oxide nucleation [*Hoffman et al.*, 2001]. Another important issue is what species are involved in the growth of these nuclei. Field measurements [*Eisele and McMurray*, 1997; *Weber et al.*, 1999; *Janson et al.*, 2001] and model simulations [*Kerminen et al.*, 2001; *Kulmala et al.*, 2001b; *Pirjola and Kulmala*, 2001; *Anttila and Kerminen*, 2003] have indicated that the condensation of sulfuric acid alone is often not sufficient to grow these nuclei to detectable sizes, since these particles have a very short lifetime before being lost through coagulation with larger existing particles. To aid in the growth of these particles, the condensation of organic species [*Kerminen et al.*, 2000], heterogeneous reactions [*Zhang and Wexler*, 2002], and ion-enhanced condensation have been suggested.

[4]   During the Pittsburgh Air Quality Study (PAQS) [*Wittig et al.*, 2004], a recent field campaign focused on elucidating aerosol sources, chemistry, and processes, ultrafine particle concentrations were monitored for 15 months. During this period, over 130 days with regional in situ new particle formation were observed. An example is shown in
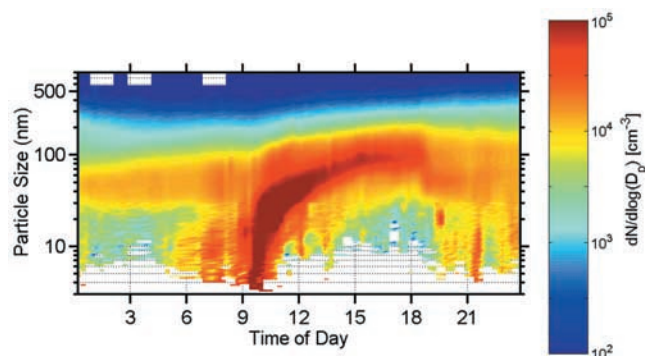
Figure 1. Evolution of the particle size distribution on 11 August 2001, a day with new particle formation and growth. Particle number concentration (z axis) is plotted against time of day (x axis) and particle diameter (y axis). A traffic signal can be seen between 0700 and 0800 EST, followed by new particle formation occurring at just after 0900 EST, and finally growth to around 100 nm in size.

Figure 1, with the smooth progression from small particle sizes at the beginning of events to larger sizes strongly suggesting a regional process.

[5] In this paper, data taken during July 2001 and January 2002 during PAQS is used to evaluate a model for the simulation of these regional nucleation events. Ternary NH_3-H_2SO_4-H_2O has been cited as an explanatory mechanism for new particle formation in several field studies, and the mechanism is used here as the core of an aerosol dynamics model to quantitatively test model-measurement agreement for new particle formation timing, strength, and evolution of size distributions. Sensitivity analysis is performed on uncertain parameters and to determine how future changes in emissions might affect nucleation, and the differences in nucleation between the summer and winter months are also explored.

2. Model Description

[6] A photochemical box model based on the framework of *Capaldo et al.* [1999] is used to model regional nucleation events occurring in July 2001 and January 2002. Atmospheric processes included in the model are gas-phase chemistry, condensation, aerosol coagulation, and nucleation. The model is a fixed sectional model with 221 size sections: 186 size sections between 3 nm and 10 μm corresponding to the measured size distribution of particles and 35 additional size sections evenly distributed in logarithmic space by diameter for particles below the detection limit of the field instruments. The concentration of SO_2 was measured directly and is an input to the model and the input concentrations of NH_3 and OH were calculated from measurement data and are discussed in section 3. The governing equations for the model, giving the change over time of the concentration of gaseous sulfuric acid, $C_{H_2SO_4}$, and the number concentration of particles in section i, N_i, are:

$$\frac{\partial C_{H_2SO_4}}{\partial t} = R_{gas}(SO_2, OH, T, P) + n^*R_{nuc}(C_{H_2SO_4}, NH_3, T, RH)$$
$$+ R_{cond}^{H_2SO_4}(C_{H_2SO_4}, RH) - R_{dep}(C_{H_2SO_4}) \quad (1)$$

$$\frac{\partial N_i}{\partial t} = R_{nuc}(C_{H_2SO_4}, NH_3, T, RH) + R_{coag}(N_j, RH)$$
$$+ R_{cond}^{N_i}(C_{H_2SO_4}, RH) - R_{dep}(N_i), \quad (2)$$

where R_{gas} is the rate of change due to gas-phase chemistry, R_{nuc} is the rate of nucleation, n^* is the number of sulfuric acid molecules in the critical nucleus, R_{coag} is the coagulation rate, R_{cond} is the condensation rate, and R_{dep} is the rate of dry deposition, with dependence on the relative humidity RH, temperature T, pressure P, dry particle size distribution, N_j, and gas-phase concentrations shown. The rate terms are discussed in detail below.

2.1. Gas-Phase Chemistry

[7] Sulfuric acid is produced from the reaction of OH and SO_2:

$$R_{gas} = k_{SO_2}[SO_2][OH], \quad (3)$$

where k_{SO_2} is the reaction constant for the reaction of SO_2 with OH from *DeMore et al.* [1994].

2.2. Nucleation

[8] The rate of nucleation, R_{nuc}, is calculated using the ternary NH_3-H_2SO_4-H_2O parameterization of *Napari et al.* [2002]. The parameterization uses the NH_3 gas-phase concentration, H_2SO_4 gas-phase concentration, temperature, and relative humidity as inputs, and provides a nucleation rate as output. The upper limit of the nucleation rate for which the parameterization is valid is 10^6 particles cm^{-3} s^{-1}, so rates higher than this are capped at this value. *Napari et al.* [2002] also give an approximation for the radius of the initial nuclei as a function of the nucleation rate and temperature. The initial nuclei diameter was calculated to be 0.8 nm for the winter and 1.0 nm during the summer, assuming average temperatures of 275 K and 298 K, respectively. The nuclei diameter was assumed to be constant for each period. The number of sulfuric acid molecules in the critical nucleus, n^*, is also calculated using the approximation given in the work of *Napari et al.* [2002]. There were roughly two sulfuric acid molecules in the critical cluster during the winter and four during the summer.

[9] Figure 2a shows the nucleation rates given by the ternary NH_3-H_2SO_4-H_2O parameterization for typical July daytime conditions: 298 K, 60% RH, and H_2SO_4 from 10^7 to 3×10^8 molecules/cm^3 (0.4 to 4.0 ppt). Ammonia is allowed to vary over the entire range of the parameterization, 0.1 to 100 ppt. The nucleation rates are not high enough for nucleation to occur unless some gas-phase ammonia is present, although ammonia concentrations above 10 ppt and sulfuric concentrations above 2.4 ppt result in nucleation rates of at least 10 particles cm^{-3} s^{-1}, so even this small amount of gas-phase ammonia can be enough for nucleation to occur on summer days in Pittsburgh.

[10] In contrast to July, where the presence of gas-phase ammonia gives the best indication of when nucleation will occur, both the H_2SO_4 concentrations and gas-phase ammonia can influence whether or not nucleation will occur during the winter. Figure 2b shows the nucleation rates for typical January conditions: 275 K, 0.7 RH, 10^5–
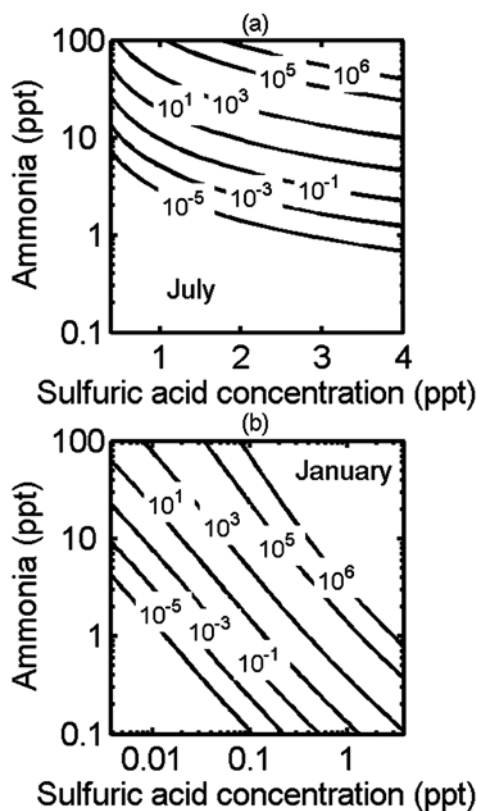
Figure 2. Nucleation rates (in particles cm^{-3} s^{-1}) for typical conditions in (a) July and (b) January. The conditions for July are: temperature 298 K, relative humidity 0.6, sulfuric acid 0.4–4 ppt, and gas-phase ammonia 0.1–100 ppt. The conditions for January are: temperature 275 K, relative humidity 0.7, sulfuric acid 0.00375–3.75 ppt, and gas-phase ammonia 0.1–100 ppt.

10^8 molecules/cm^3 H_2SO_4 (0.00375 to 3.75 ppt), and 0.1–100 ppt NH_3. At higher sulfuric acid concentrations, nucleation rates can still reach about 1000 particles cm^{-3} s^{-1} even with very low gas-phase ammonia concentrations. At lower sulfuric concentrations, nucleation rates can be less than 100 cm^{-3} s^{-1} even with high gas-phase ammonia concentrations. Consequently, the amount of H_2SO_4, which varies more than in the summer months, plays a more important role during the winter.

2.3. Condensation

[11] The condensation rate, R_{cnd}, is described using the modified form of the Fuchs-Sutugin equation [*Fuchs and Sutugin*, 1971; *Hegg*, 1990; *Kreidenweis et al.*, 1991]. The condensation rate J to a particle of diameter D_p is given by:

$$J = 2\pi D D_p F(Kn)A(p - p_0), \qquad (4)$$

where D is the diffusivity of sulfuric acid in air (set to 0.1 cm^2 s^{-1}), Kn is the Knudsen number, and $F(Kn)$ is a coefficient correcting for free molecular effects:

$$F(Kn) = \frac{1 + Kn}{1 + 1.71Kn + 1.33Kn^2}. \qquad (5)$$

A is a coefficient correcting for the interfacial mass transport limitations described by the accommodation coefficient a_e:

$$A = \left[1 + 1.33KnF(Kn)\left(\frac{1}{a_e} - 1\right)\right]^{-1}. \qquad (6)$$

Here p is the bulk partial pressure of sulfuric acid and p_0 is its partial pressure at the particle surface. The value of the accommodation coefficient depends on the composition of the particle, with the presence of organic species in the aerosol likely to result in a lower accommodation coefficient. *Jefferson et al.* [1997] report values of 0.31 and 0.19 for the accommodation coefficient onto a NaCl aerosol coated with stearic acid with high and low coverage, respectively, compared to values 0.73 ± 0.21 for ammonium sulfate particles and 0.79 ± 0.23 for NaCl. Since the preexisting aerosol mass is likely to be a mixture of inorganic and organic species, the accommodation coefficient is set at 0.2 in this work. Sensitivity analysis is performed to see how changes in this parameter affect the model results.

[12] H_2SO_4 is assumed to be the major condensing species. Although it is likely that other species, such as nitrate, ammonium, and organic compounds, also are involved in the growth of the nuclei, their respective roles remain unclear. Measurements taken during PAQS in September 2002 indicate that sulfuric acid is the primary initial species involved in the growth of the nuclei, followed by ammonium and then organics, whose presence lags behind sulfuric acid by .5 hours to up to 2.5 hours in the smallest measured particles (AMS measurements of particles 22–40 nm, estimated physical diameter) [*Zhang et al.*, 2004]. Although contributions of other species cannot be ruled out, condensation of sulfuric acid alone produces growth that is similar to the observations, as will be discussed in more detail below.

[13] The vapor pressure of sulfuric acid at the surface of the aerosol can be estimated from the data of *Bolsaitis and Elliott* [1990]. For example, at a temperature of 293 K and a relative humidity of 90%, the value of p_0 is approximately 10^{-5} ppt. Since the calculated values of p_0 are much smaller than ambient sulfuric acid concentrations, p_0 is assumed to be zero.

[14] For the ith aerosol size section from $x_i = \log_{10}(D_i)$ to $x_{i+1} = \log_{10}(D_{i+1})$, the sulfuric acid condensation rate is given by

$$J_i = K_{mt}^i N_i C_{H_2SO_4}, \qquad (7)$$

where the sectional mass transfer coefficients K_{mt}^i are calculated by

$$K_{mt}^i = \frac{2\pi D}{x_{i+1} - x_i} \int_{x}^{x_{i+1}} 10^x F(x)A(x)dx. \qquad (8)$$

The total change in the gas-phase concentration of sulfuric acid due to condensation is equal to the sum of J_i over all size sections i.

[15] The diameter of the aerosol particle is adjusted to be in equilibrium with the ambient RH before the calculation.

The dry aerosol diameter, $D_{p,dry}$, is increased due to the addition of water vapor according to the following parameterization for ammonium bisulfate based on data presented by *Seinfeld and Pandis* [1998]:

$$\frac{D_{p,wet}}{D_{p,dry}} = 17.8(RH - 50\%)^{3.5} + 1.28. \qquad (9)$$

The parameterization is valid for RH between 50% and 98%. When RH is below 50%, the particles are assumed to have negligible amounts of water. This parameterization neglects the effect of curvature, which can be significant for particles less than 10 nm in size.

[16] Finally, the change in the number concentration in section i, N_i, is calculated from the relation:

$$R_{cond}^{N_i} = F_{i-1}N_iC_{H_2SO_4} - F_iN_iC_{H_2SO_4}, \qquad (10)$$

where F_i is the flux from section i into section i + 1:

$$F_i = \frac{6M_{H_2SO_4}K_{mt}^iD_{p,wet}}{RT\rho\pi\left[\left(D_{p,dry}^{i+1}\right)^3 - \left(D_{p,dry}^i\right)^3\right]}. \qquad (11)$$

$M_{H_2SO_4}$ is the molecular weight of sulfuric acid, ρ is the density of the particles, and R is the ideal gas constant.

2.4. Coagulation

[17] The coagulation rate of aerosol particles, R_{coag}, is modeled according to *Seinfeld and Pandis* [1998], using linear interpolation to preserve both mass and particle number concentrations:

$$R_{coag} = \frac{1}{2}\sum_{j=1}^{k}f_kK_{j,k-j}N_jN_{k-j} - N_k\sum_{j=1}^{\infty}K_{k,j}N_j, \quad k \geq 2 \qquad (12)$$

where $K_{k,j}$ is the coagulation coefficient of particles in section k and j, and f_k is a correction factor to preserve mass, giving the fraction of the newly formed particle that will go into section k. The generalized coagulation coefficient for the collision of two particles is defined as:

$$K_{12} = 2\pi(D_{p1} + D_{p2})(D_1 + D_2)\beta, \qquad (13)$$

where β is the Fuchs correction factor [*Fuchs*, 1964]. Linear interpolation is then used to determine the value of f_k. For example, if V_p is in between sections k and $k + 1$, with volumes V_k and V_{k+1} respectively, then f_k is defined as:

$$f_k = \frac{V_{k+1} - V_p}{V_{k+1} - V_k}, \qquad (14)$$

$$f_{k+1} = \frac{V_p - V_k}{V_{k+1} - V_k}. \qquad (15)$$

2.5. Dry Deposition

[18] Dry deposition is modeled using a species and aerosol size-dependent deposition velocity, v_{dep}, such that

$$R_{dep} = \frac{v_{dep}c_i}{H}, \qquad (16)$$

where c_i is the concentration of gas species or aerosol size section i, and H is the mixing height. Aerosol dry deposition rates range from 0.1 to 0.015 cm s^{-1} dependent on particle size according to *Hummelshoj et al.* [1992] while the deposition velocity of H$_2$SO$_4$ is assumed to be 1.0 cm s^{-1} [*Brook et al.*, 1999].

3. Simulation Inputs

[19] Meteorological data, gas-phase concentrations, and aerosol number concentrations were available as inputs for these time periods from ground-level observations during the Pittsburgh Air Quality Study (PAQS) [*Wittig et al.*, 2004]. Temperature, relative humidity, and UV radiation are updated from 15-min averages during July, and 10-min averages during January. SO$_2$ concentrations are averaged over 10-min intervals for both months. Initial aerosol number distributions are available from dry size distributions measured every 15 min [*Stanier et al.*, 2004a]. Each simulation starts sometime between 0000 and 0900 (depending on meteorology), and ends at midnight.

3.1. Gas-Phase Ammonia Concentrations

[20] Gas-phase NH$_3$ was not measured directly during this period and was estimated from related quantities using two independent methods. First, total NH$_3$ (PM$_{2.5}$ ammonium + NH$_3$(g), sampled hourly during July and every 2 hours during January using a steam sampler [*Khylstov et al.*, 1995] and quantified by ion chromatography) was compared to the particulate sulfate and nitrate. Hourly particulate sulfate and nitrate concentrations are composites of measurements made using several methods, including filter-based and semicontinuous methods [*Wittig et al.*, 2004]. If enough NH$_3$ was present to fully neutralize the particulate sulfate and nitrate, then the excess NH$_3$ was assumed to be in the gas phase. Second, total NH$_3$, total nitrate and sulfate (all from steam sampler/ion chromatography) were assumed to be in thermodynamic equilibrium, with gas and particulate phase concentrations determined by the model GFEMN [*Ansari and Pandis*, 1999]. The two methods showed excellent agreement for the time periods studied.

3.2. OH Concentration

[21] To estimate the OH concentration, a maximum value is assumed for both July and January, and then this value is scaled linearly based on the 15-min average measured UV radiation. The summer maximum was chosen as 5 × 10^6 molecules/cm^3. Observations in New York City during July 2001 had an average maximum OH concentration of 7 × 10^6 molecules/cm^3 [*Ren et al.*, 2003a, 2003b] and other measurements during the summer months have given maximum OH concentrations in a similar range [*Tan et al.*, 2001; *Creasey et al.*, 2002; *Mauldin et al.*, 2001; *George et al.*, 1999]. Fewer studies have been done in the winter, although *Heard et al.* [2001] have compared measurements
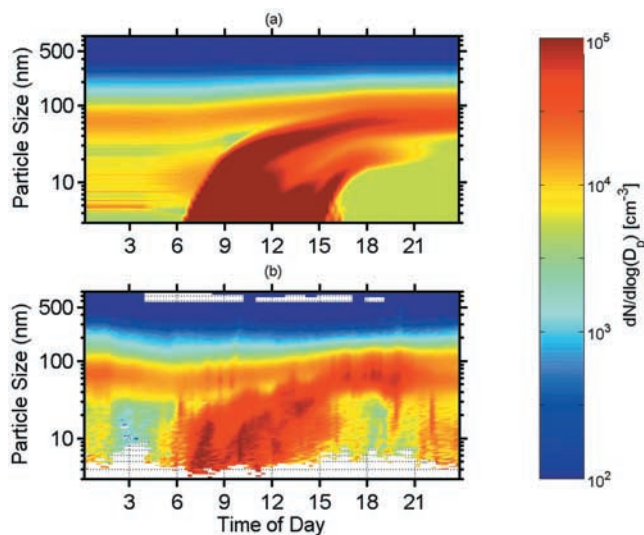
Figure 3. Comparison of modeled (a) and measured (b) size distributions as a function of time for one day with nucleation activity (27 July 2001). Particle number (z axis) is plotted against time of day (x axis) and particle size (y axis). The increased number concentrations observed between 0600 and 0700 EST and after 2100 EST are due to local emissions of ultrafine particles. The observed onset of nucleation at ∼0700 EST is captured in the model, and the qualitative features of particle growth are also captured by the model.

taken in Birmingham, England during June 1999 and January 2000. They reported that winter OH noontime maximum concentrations in Birmingham ranged from $0.6-5 \times 10^6$ molecules/cm^3. Although the ozone photolysis was around 20 times lower compared to July, these winter OH concentrations were on average only $2-3$ times lower than in the summer, where the noontime maxima ranged from $3-8 \times 10^6$ molecules/cm^3. In this paper, a base case value of 1×10^6 molecules/cm^3 is used for the January simulations, a factor of 5 different from July. Sensitivity analysis is performed on both the summer and winter maxima to assess how these assumptions affect the results.

3.3. Local Emissions of Ultrafine Particles

[22] From the measurements, it is clear that there are a number of local sources of ultrafine particles which affect the observed number concentrations. The most prominent local source is automobile traffic, which is strongest during morning rush hour between 0600 and 0900 EST. On the basis of the observations, these local emissions appear to have little effect on the regional nucleation events, which usually begin after the morning traffic has returned to normal levels. Even when there are relatively high numbers of ultrafine particles present when nucleation occurs, the number of particles produced by nucleation is much greater than from local sources, and the smooth growth of these nucleated particles is the dominant behavior observed. The fresh particles from these local sources have a relatively low surface area, and they do not appear to have much effect on the nucleation either through depletion of gaseous sulfuric acid concentrations or through coagulation with the nucle-

ated particles. Because of this, these local sources of ultrafine particles can be ignored as a first approximation.

4. Observations

[23] Overall, significant new particle formation was observed on seventeen days during July 2001. Twelve days of July 2001 were not modeled due to missing measurement data (8 days), local primary source influences (3 days), and meteorology that severely violated the box model assumptions (1 day). Of the 19 days modeled, nucleation occurred on 13 of them, while there was no evidence of new particle formation on the other 6. Most of the nucleation events in July started at about 0900 EST, just a few hours after sunrise. Nucleation also tends to occur on days with below average PM$_{2.5}$ concentrations and clear skies [*Stanier et al.*, 2004b]. Many of these events are regional in nature, taking place over several hours with smooth growth, indicating that nucleation is taking place over a large geographic area. The events are observed to sometimes coincide with mixing of the stable nighttime ground-level atmosphere. This is similar to observations of nucleation coincident with atmospheric mixing seen in Germany [*Birmili et al.*, 2003] and Finland [*Nilsson et al.*, 2001] and suggests that vertical mixing can be important to nucleation. However, a significant fraction of nucleation events observed in Pittsburgh did not coincide with atmospheric mixing, and occurred either earlier or later than the rise in boundary layer height [*Stanier et al.*, 2004b]. The degree to which vertical transport is important to nucleation in the eastern United States is currently unknown and vertical transport is not included in the box model developed here.

[24] In January, 19 days had no observed nucleation. The first 2 days of the month cannot be modeled because of missing data, leaving 17 days with no nucleation and 12 days where nucleation was observed in our data set. Nucleation typically began around noon, presumably once sufficient sulfuric acid was produced for nucleation and growth to occur. The nucleation events tended to be weaker and shorter-lived than during the summer months, and particles did not grow as much. This is consistent with lower levels of sulfuric acid (predicted by the model) and lower secondary organic aerosol during the winter [*Cabada et al.*, 2002].

5. Results
5.1. Base Case

[25] An example simulation is shown for 27 July 2001, when new particle formation occurred over a 9-hour span (Figure 3), beginning shortly after 0600 and continuing to nearly 1500 EST. The model prediction compares well with the observed behavior, with the timing of the event and the size and shape of the growth curve similar to the observations. The model does predict higher number concentrations, however, producing a peak hourly average of 93,000 cm^{-3} for particles greater than 10 nm in diameter, compared to a maximum of 47,000 cm^{-3} from the measurements, and the model-predicted nucleation is also stronger between noon and 1500 EST.

[26] As shown in Table 1, the model successfully predicted the presence or lack of new particle formation on all

Table 1. Predicted and Observed New Particle Formation During July 2001

Day of July 2001	Observed Strength of Nucleation[a]	Time of Nucleation, EST		Final Mode Diameter of Nucleation Mode, nm		Daily Average Number Concentration > 10 nm, 10^3 cm^{-3}		Peak Hourly Number Concentration > 10 nm, 10^3 cm^{-3}	
		Observed	Predicted	Observed	Predicted	Observed	Predicted	Observed	Predicted
1	moderate	0900	0800	20	60	10	53	19	158
2	weak	0800	0800	80	60	21	50	32	150
3	weak	0900	0900	10	65[b]	17	50[b]	22	184[b]
4	none	none	none	–	–	9	6	12	8
6	weak	0900	0900	60	65	24	54	42	159
7	none	none	none	–	–	12	13	26	20
8	none	none	none	–	–	11	10	18	11
9	strong	1000	0900	90	100	24	73	54	259
11	moderate	0900	0900	40	50	24	35	47	105
12	moderate	0900	0900	70	60	21	59	37	164
13	weak	0900	0900	50	40	19	37	27	86
14	strong	0800	0900	60	60	19	46	36	127
15	moderate	0800	0900	50	60	25	48	44	145
18	none	none	none	–	–	16	10	24	18
19	none	none	none	–	–	11	7	17	17
23	none	none	none	–	–	8	9	16	17
24	moderate	0800	0800	70	80	19	47	44	170
26	moderate	1600	1700	40	20	17	31	35	108
27	strong	0600	0600	70	70	28	45	47	140

[a]Events were classified as no new particle formation, weak, moderate, or strong according to the observed rate of change of particle number between 3 and 10 nm. Strong events have $dN_{10}/dt > 15,000$ cm^{-3} hr^{-1}, moderate events from 4000 to 15,000, and weak events between 2000 and 4000 cm^{-3} hr^{-1}. No new particle formation refers to a dN_{10}/dt that was not distinguishable from the natural variability in nuclei mode particle concentrations due to local primary sources. Usually the noise threshold was about 2000 cm^{-3} hr^{-1}.

[b]Multiple air masses moved through the region on this day, probably violating the box model assumptions. This day was modeled to see if the observed 0900 burst in number concentration was replicated by the model, rather than to compare the observed and modeled growth.

19 modeled days in July. The timing of the events also compared well with the observations, with the model predicting the start of new particle formation within 1 hour for all 13 events. The size and shape of the growth curve were consistent with measurements, with the predicted average final size of the nucleated particles within 10 nm of the actual size in 9 out of the 13 nucleation days. Three of the days with poor agreement are days where observed growth is significantly less than the majority of days. Two of these days (the 1st and 3rd) are characterized by fronts moving through the region, which could effect the performance of the model, and on the other day nucleation is delayed until late afternoon because of cloud cover (26th).

[27] A strong correlation between the presence of free NH$_3$ in the gas phase and new particle formation contributed to the success of the model in July. During the 13 days where particle production was observed, gas-phase NH$_3$ concentrations exceeded 100 ppt while nucleation was occurring. Although Pittsburgh has a high average sulfate concentration, on the 13 days in question there was sufficient NH$_3$ to neutralize the aerosol sulfate. In contrast, during the 6 days without new particle formation, the aerosol sulfate levels were higher, leaving less NH$_3$ in the gas-phase (typically a few ppt). Other parameters, such as SO$_2$, temperature, relative humidity, and UV radiation, all varied widely over the nineteen days. The preexisting surface area tended to be less on the days with particle formation than those without, although there was some overlap.

[28] The ternary NH$_3$-H$_2$SO$_4$-H$_2$O parameterization is also successful in predicting the presence of nucleation in January (Table 2). Peak and average number concentrations are not shown for the month of January because the local sources of ultrafine particles occasionally produce similar

number of particles as the nucleation events, which produce fewer particles than in July. The difference between particles produced by these local sources and the nucleation events is clear, however, and there appears to be no interaction between the particles produced by these different phenomena. The model is successful in predicting 11 of the 12 observed events, with the exception being the 14th. This day has a sudden drop in surface area shortly after the observed nucleation begins, which is difficult to capture in the model. The model also suffers from three "false positive" cases in January, predicting nucleation events on 3 days where it was not observed in the field. Two of these predicted events are very weak and do not exhibit growth above 10 nm (the 24th and 29th), while the particles from the third additional event grow only to 15 nm in size.

[29] A comparison of the model prediction and observations for 28 January 2002 is shown in Figure 4. The predicted onset of nucleation compares well with the observations, beginning shortly after noon. The predicted nucleation event lasts about 1.5 hours longer, and produces more particles than observed. This overprediction of number concentrations is typical in January, as it was in July. In addition, the overall timing of the events does not agree as well as in July, with one event predicted to occur 3 hours earlier than the observed event (on the 9th) and two other events occurring at least 2 hours before nucleation is observed. Most of the predicted nucleation events show growth that is similar or less than the observed growth, although two events show considerably more growth than observed (the 18th and 22nd).

[30] The good agreement with the growth of the particles is somewhat surprising, with sulfuric acid as the only condensing species included in the model. However, due the cubic relation between diameter and volume seemingly

Table 2. Predicted and Observed New Particle Formation During January 2002

Day of January 2002	Observed Strength of Nucleation	Time of Nucleation, EST		Final Mode Diameter of Nucleation Mode, nm	
		Observed	Predicted[a]	Observed	Predicted[a]
3	none	-	-	-	-
4	none	-	-	-	-
5	weak	1200	1100	20	20
6	none	-	-	-	-
7	none	-	-	-	-
8	none	-	-	-	-
9	weak	1200	1200	30	20
10	none	-	-	-	-
11	none	-	-	-	-
12	weak	1300	1000	30	20
13	moderate	1200	1330	25	15−20
14	weak	1100	-	20	-
15	none	-	-	-	-
16	none	-	-	-	-
17	none	-	-	-	-
18	weak	1300	1330	8	10−15
19	none	-	1100	-	10−15
20	none	-	-	-	-
21	none	-	-	-	-
22	moderate	1200	0930	25	40
23	none	-	-	-	-
24	none	-	1330	-	10
25	strong	1130	1000	30	25
26	strong	0915	1000	25	25
27	strong	1100	1030	30	20
28	moderate	1200	1230	25	20
29	none	-	1300	-	8
30	none	-	-	-	-
31	weak	1200	1000	10−15	15

[a]To classify as an event, the predicted nucleation had to last for at least an hour and produce particles that grew to at least 8 nm in size (the smallest size for an observed event). Events that do not meet these criteria would probably not be observed.

large differences in mass will not greatly affect the diameter. For example, AMS measurements indicate that the final mode of the particles (around 100 nm) for three measured events in September 2002 are approximately 25%, 25%, and 40% organic by mass [*Zhang et al.*, 2004]. Leaving out this organic mass would result in a reduction of only 9% to 16% in the final diameter of the particles. Thus it is possible that organic and other inorganic species are also involved in the growth, although sulfuric acid alone appears to be sufficient to grow the particles to significant sizes in Pittsburgh during the periods studied.

5.2. Sensitivity to Changes in the Maximum OH

[31]   One of the major uncertainties in the model is OH concentration. The July simulations were repeated with maximum OH concentrations of 10^7 molecules/cm^3 (200% of the base case value) and 2.5×10^6 molecules/cm^3 (50% of the base case value). No change was seen in the number of nucleation events for either of these additional cases, with the model still predicting nucleation to occur on the same 13 days (68% of the modeled days). The growth of the particles changed significantly, however. A maximum OH concentration of 10^7 molecules/cm^3 resulted in significantly more growth than in the base case simulations. For 12 of the 13 events, the nucleated particles grew to at least 80 nm, with the final mode of nine of these events at least 100 nm in size. With a maximum OH concentration of 2.5×10^6 molecules/cm^3, the final mode size of the nucleated particles is 20% less than for the base case on average.

[32]   In January, both the number of nucleation events and the growth of the nucleated particles are sensitive to changes in the maximum OH concentration (Table 3). Again, the simulations are performed with OH levels 200% of the base
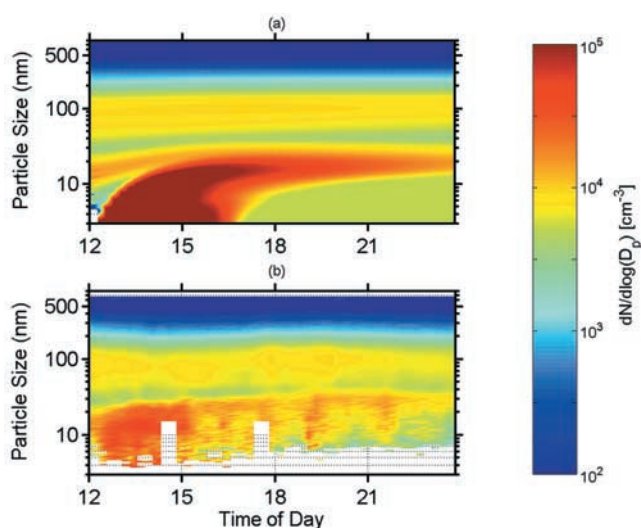

Figure 4. Comparison of modeled (a) and measured (b) size distributions as a function of time for a day in January with nucleation activity (28 July 2001). Particle number (z axis) is plotted against time of day (x axis) and particle size (y axis).

Table 3. OH Sensitivity Analysis for January 2002

Day of January 2002	OH, 0.5×10^6 molecules/cm^3		OH, 1×10^6 molecules/cm^3 (Base Case)		OH, 2×10^6 molecules/cm^3	
	Time, EST	Final Mode	Time, EST	Final Mode	Time, EST	Final Mode
3	-	-	-	-	-	-
4	-	-	-	-	1100	25
5	-	-	1100	20	0930	45
6	-	-	-	-	-	-
7	-	-	-	-	-	-
8	-	-	-	-	1200	15
9	1200	10	1200	20	1100	30
10	-	-	-	-	-	-
11	-	-	-	-	-	-
12	1000	10	1000	20	0900	35
13	1300	10	1330	15–20	1330	25
14	-	-	-	-	1100	9
15	-	-	-	-	1300	10
16	-	-	-	-	1100	15
17	-	-	-	-	1030	20
18	-	-	1330	10–15	1300	25
19	-	-	1100	10–15	1030	25
20	-	-	-	-	1030	15
21	-	-	-	-	1000	15
22	1000	20	1000	40	0900	55
23	-	-	-	-	-	-
24	-	-	1330	10	1300	20
25	1100	10	1000	25	0930	45
26	1200	15	1000	25	0930	45
27	1130	10	1030	20	1030	40
28	1230	9	1230	20	1200	30
29	-	-	1300	8	0900	20
30	-	-	-	-	1000	10
31	-	-	1030	15	1000	30

case value (a maximum of 2×10^6 molecues/cm^3) and 50% of the base case value (5×10^5 molecules/cm^3). The number of events predicted ranges from 8 with OH levels 50% of the base case (28% of the modeled days) to 21 with OH levels 200% of the base case (72% of the days). The growth of the nucleated particles is significantly greater with a maximum OH concentration of 2×10^6 molecules/cm^3, with 16 events having particles grow to at least 20 nm in size, compared to 8 for the base case. With a maximum OH concentration of 5×10^5 molecules/cm^3, particles from only 2 of the 8 events grow above 10 nm in size, and only 1 event exhibits growth to 20 nm. The difficulties of the model in the simulation of a few winter days could be due to this sensitivity to the uncertain OH concentration. Because of the sensitivity of nucleation in January to the maximum OH concentrations, additional field measurements of OH would help to improve our understanding of nucleation during the winter months.

5.3. Sensitivity to Accommodation Coefficient

[33] Another source of uncertainty is the value of the accommodation coefficient. In addition to the base case value of 0.2, simulations were run with the accommodation coefficient set to values of 0.5 and 1.0. Higher values of the accommodation coefficient will tend to increase the uptake of sulfuric acid onto the preexisting aerosol mass, lowering the gaseous sulfuric acid concentrations (and, consequently, the nucleation rates). The higher accommodation coefficient also has the potential to increase the growth of the nucleated particles, despite the lower sulfuric acid concentrations.

[34] In July, the average predicted sulfuric acid concentrations are reduced by a factor of 2 for an accommodation

coefficient of 0.5, and 3 for an accommodation coefficient of 1.0. The corresponding reductions in the nucleation rate are 22%, and 31%, respectively. However, with the presence of ammonia as the major factor in determining when nucleation occurs in July, the number of days which exhibit nucleation does not change. The final mode of the nucleated particles increases by about 5 nanometers for 2 of the 13 events with an accommodation coefficient of 0.5, and for 5 of the 13 events with an accommodation coefficient of 1.0.

[35] In January, changes in the accommodation coefficient had mixed effects, although the number of events was not affected. The average sulfuric acid concentrations between 1000 and 1400 are reduced by a similar amount, a factor of 2 for an accommodation of coefficient of 0.5, and a factor of 3 using a value of 1.0. The nucleation rates are reduced by 8% and 15%, respectively. The reduction does not affect the number of events. With an accommodation coefficient of 0.5, four events are either shorter, weaker, or exhibit less growth than for the base case, while three events produced particles that grew larger than in the base case. Using an accommodation coefficient of 1.0 in the model, five events exhibit more growth than the base case, while four events are either weaker, shorter, or exhibit less growth. The final mode of the nucleated particles was within 5 to 10 nm of the base case in all cases.

5.4. Binary Nucleation

[36] Several binary (H_2SO_4-H_2O) parameterizations were also used in the model for comparison. The parameterization of *Vehkamäki et al.* [2002] predicted no nucleation events in either the summer or winter. Comparisons with
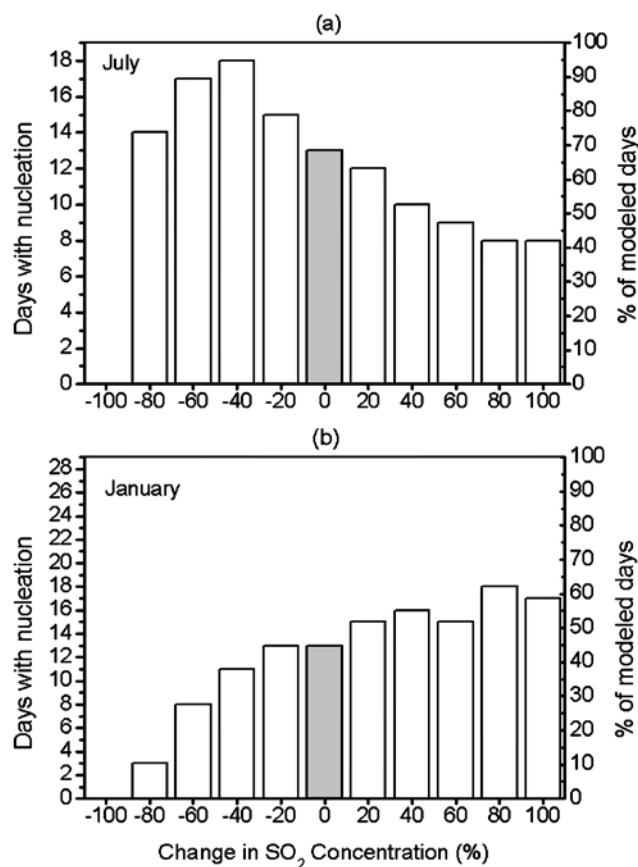
Figure 5. Sensitivity to changes in SO_2 concentrations for (a) July and (b) January. The shaded bars represent the base case scenario.

nucleation thresholds given by *Wexler et al.* [1994] and *Pirjola et al.* [1999] also revealed that estimated sulfuric acid concentrations were below the threshold needed for H_2SO_4-H_2O nucleation to occur in both months at the relative humidity and temperature corresponding to the ground level, as well as the top of the mixed layer [*Stanier et al.*, 2004b]. Finally, the parameterization of *Jaecker-Voirol and Mirabel* [1989] was applied, both with and without a nucleation tuner. Without the tuner, no nucleation events were predicted. Although there is a lot of uncertainty as to what value to use for the tuner, *Raes et al.* [1992] have suggested a value of between 10^4 to 10^7 to bring the results into better agreement with measurements. Even with a value of 10^7, however, only four nucleation events were predicted in January, and no events were predicted in July.

[37] The poor performance of the binary models is consistent with results by other researchers who have found that sulfuric acid concentrations are generally not high enough to induce binary nucleation in the lower troposphere [*Korhonen et al.*, 2003; *Kulmala et al.*, 2002; *Weber et al.*, 1996, 1999]. In fact, the predicted sulfuric acid concentrations are similar on days with and without nucleation for both the summer and winter simulations. In July, the average sulfuric acid concentration on days with nucleation is 6.5×10^7 molecules/cm^3 between 0900 and 1500 EST, about 10% less than the corresponding value of 7.2×10^7 molecules/cm^3 on days without nucleation.

The daily maximum concentrations predicted for July are 2.8×10^8 and 2.9×10^8 molecules/cm^3 on days with and without nucleation, respectively, while the concentrations are generally at least 10^7 molecules/cm^3. In January, the average sulfuric acid concentration on days with nucleation (1.8×10^7 molecules/cm^3) is about 30% higher than on days without nucleation (1.3×10^7 molecules/cm^3). The maximum sulfuric acid concentrations are again similar, 1.3×10^8 and 1.4×10^8 molecules/cm^3, respectively, while the predicted concentrations are generally above 10^5 molecules/cm^3.

6. Effect of Changes in SO_2 and NH_3 Emissions

[38] Sensitivity analysis was also performed to determine how changes in emissions of SO_2 and NH_3 would influence nucleation during summer and winter conditions. Scenarios were modeled changing the emissions of one gas while leaving the other at the base case level, as well as with both ammonia and SO_2 being simultaneously controlled. The following changes were made to the model inputs with changes in SO_2 emissions: (a) a proportional change was made in the gas-phase SO_2 and aerosol sulfate concentrations; (b) the gas-phase ammonia concentrations were recalculated using the adjusted aerosol sulfate concentrations and conserving the total ammonia; (c) the initial surface area was reduced proportional to the change in total aerosol mass. Changes in aerosol mass are calculated accounting for the change in sulfate concentrations, the mass fraction of sulfate in the aerosol phase, and adjusting for replacement of sulfate by nitrate and ammonium when sufficient NH_3 and HNO_3 are available [*Seinfeld and Pandis*, 1998]. The adjustment to the surface area implicitly assumes that there is no change in the shape of the aerosol distribution. In reality, there would be a shift in the distribution with changes in total mass. However, sensitivity analysis on the preexisting surface area showed that the results were insensitive to changes of up to 20% (the number of events remains the same while the growth of nucleated particles is affected only slightly), so the error introduced by this simplifying assumption can be ignored. Changes in NH_3 emissions are handled in a similar manner: (a) the total ammonia is changed proportionally to the change in NH_3 emissions; (b) the gas-phase ammonia concentrations are recalculated with the new values for total ammonia; (c) the initial surface area is adjusted proportionately to the change in aerosol mass resulting from the increase of total ammonia.

[39] Figure 5 shows the effects of changes in SO_2 emissions for both the January and July simulations. For the July simulations, increasing the SO_2 emissions decreases the number of nucleation events, as the additional aerosol sulfate lowers the amount of gas-phase ammonia and reduces the nucleation rates. The fresh particles that are created grow to larger sizes, however, as there is more sulfuric acid being produced to contribute to the growth of the particles. Lowering SO_2 emissions initially increases the number of nucleation events, as gas-phase ammonia concentrations increase and raise the nucleation rates. A maximum of 18 events out of the 19 modeled days occurs with a 40% reduction in SO_2. Additional reductions in SO_2 decrease the number of nucleation events and substantially
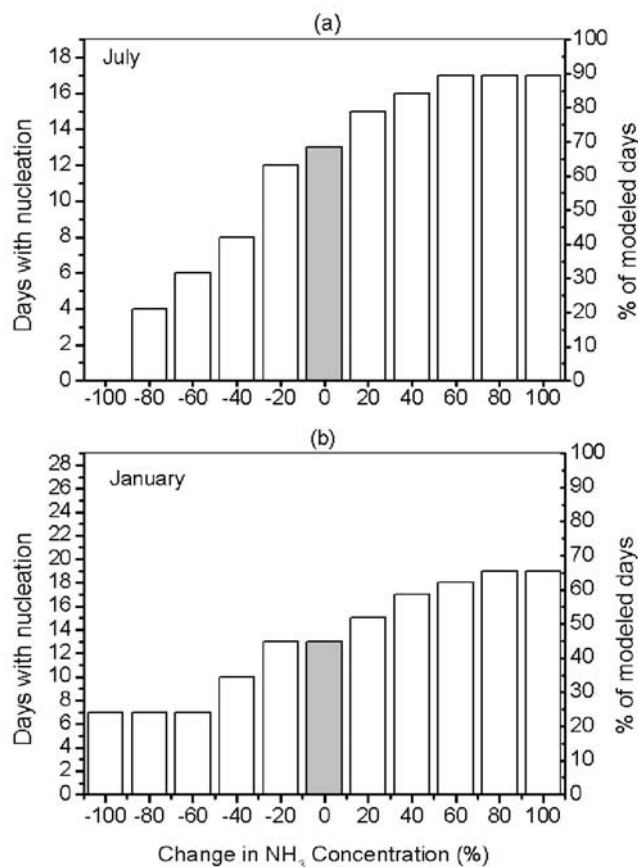
Figure 6. Sensitivity to changes in ammonia emissions for (a) July and (b) January. The shaded bars represent the base case scenario.

reduce the amount of growth seen. Even with an 80% reduction in SO_2 emissions, however, fourteen nucleation events occur (74% of the modeled days), although eight of these events are very weak with the nucleated particles not growing above 20 nm in size.

[40] In January, changes in SO_2 emissions have the opposite effect, with increases in SO_2 emissions tending to cause additional events, and vice versa. This is indicative of the fact that sulfuric acid, in conjunction with ammonia, plays an important role in determining the nucleation rate in January, as opposed to in the summer when ammonia controls the system. The model predicts a maximum of 18 events (62% of the modeled days) with an 80% increase in SO_2 emissions, 5 more than for the base case. The nucleation events also exhibit increased growth as the SO_2 emissions are increased. With a 40% reduction in SO_2, nucleation is still seen on 38% of the days, although the particles from only 2 of the 11 events grow to 20 nm in size. An 80% reduction in SO_2 leaves only 3 events (10% of the modeled days), with the mode of the particles only reaching 10 nm in size for all three events.

[41] In July, a strong positive correlation is seen between changes in total ammonia and the number of nucleation events (Figure 6). In July, the model predicts 17 events when the total ammonia is increased by more than 60% (89% of the modeled days). A 40% reduction in ammonia eliminates 5 nucleation events seen in the base case (leaving

42% of the days showing nucleation), while a 100% reduction eliminates all the events. The length of the nucleation events is also affected as ammonia decreases, with several of the events becoming significantly shorter.

[42] Although a similar trend is seen in January, ammonia does not have as great an effect as in July. Even with a 100% reduction in total ammonia, seven events still occur (24% of the modeled days), with the particles from 5 of these events growing to at least 20 nm in size. For these cases, the lower limit of ammonia for the parameterization was used, 0.1 ppt, so these cases do not reduce to the binary H_2SO_4-H_2O case. A doubling of ammonia results in nineteen predicted nucleation events (66% of the days), although 8 of these events are weak and do not exhibit growth above 20 nm in size.

[43] Although SO_2 emissions have been reduced substantially since the 1980s by the Clean Air Act, further reductions are planned [e.g., *U.S. Congress*, 2003] to help reduce fine particulate matter mass concentrations in the eastern United States, which have been linked to adverse health effects [*Samet et al.*, 2000; *U.S. Environmental Protection Agency*, 1996]. With these further reductions in SO_2 already planned, additional scenarios were simulated for July in which NH_3 was controlled in addition to SO_2. As shown previously, a 40% reduction in sulfate results in five additional events during this month. When coupled with a 10% reduction in NH_3, however, three of these additional events are eliminated. A reduction of NH_3 by 30% eliminates the other two additional events, leaving just the original thirteen.

7. Conclusions

[44] A strong correlation between the presence of gas-phase ammonia in July and observed nucleation indicates that ternary NH_3-H_2SO_4-H_2O nucleation is the likely mechanism for nucleation in Pittsburgh. The ternary NH_3-H_2SO_4-H_2O nucleation parameterization of *Napari et al.* [2002] is shown to accurately predict the presence or lack of nucleation during both the summer and winter: 19 out of 19 days in July, and 25 out of 29 days in January. The success of the model using H_2SO_4 as the sole condensing species and without simulating the effect of organics suggests that the role of organics in the formation and growth of these nucleated particles is probably secondary.

[45] The predicted size and shape of the growth curve, as well as the timing of the onset of nucleation, is in good agreement with observations, particularly in July. The predicted timing of the events is within 1 hour of the observations for all 13 events in July, and 6 of the 12 events in January. Nine of the thirteen predicted events show very similar growth compared to the observations in July, while the model generally predicts less growth than observed in January. The model tends to predict higher number concentrations of particles on days with nucleation for both the summer and winter months. In July, for example, the predicted daily average and peak hourly number concentrations of particles larger than 10 nm are 2.5 and 4.3 times higher, respectively, than the observed number concentrations on these days. Although this discrepancy in number concentrations might be partially explained by the model not accounting for coagulational

scavenging of particles smaller than the critical cluster as well as dilution as the mixing layer rises during the day, this issue needs to be further explored.

[46] Sensitivity analysis on the OH concentrations reveals that the number of nucleation in July events is insensitive to the OH concentration, while the number of events in January ranges from 8 (28% of the modeled days) with OH concentrations 50% of the base case value to 21 (72% of the days) with OH concentrations twice the base case value. The growth of the nucleated particles due to sulfuric acid condensation changes significantly for both months as a function of the assumed maximum OH. Field measurements of OH concentrations during the winter months would greatly enhance our understanding of nucleation during the winter.

[47] Additional sensitivity analysis shows what effect future changes in ammonia and SO_2 emissions would have on the number and strength of nucleation events. In both July and January, the number of events shows a strong correlation with ammonia emissions. In July, reducing the ammonia emissions by 100% eliminates all the nucleation events, while doubling ammonia emissions results in 17 events (89% of the modeled days). In January, the relationship is not quite as strong, with the percentage of days exhibiting nucleation rising from 24% with no ammonia to 66% with double ammonia. The effect of changes in SO_2 emissions is different depending on the season. In January, there is again a positive correlation with the number of events. An 80% reduction in SO_2 emissions leaves only 3 events, while doubling the SO_2 results in 19 events (66% of the days). In July, the simulated effect of SO_2 emissions is nonlinear. For the July simulations, SO_2 reductions can either increase or decrease the frequency of nucleation. Reductions up to about 40% will increase the number of days with nucleation, while larger reductions will ultimately decrease the frequency. Doubling the SO_2 in summer decreases the nucleation frequency substantially. Like the changes in OH concentrations, the amount of SO_2 also affects the growth of the nucleated particles significantly in both months, as the amount of sulfuric acid available for condensation is affected.

References

Adams, P. J., and J. H. Seinfeld (2003), Disproportionate impact of particulate emissions on global cloud condensation nuclei concentrations, *Geophys. Res. Lett.*, 30, 1239, doi:10.1029/2002GL016303.

Ansari, A. S., and S. N. Pandis (1999), Prediction of multicomponent inorganic atmospheric aerosol behavior, *Atmos. Environ.*, 33, 745–757.

Anttila, T., and V.-M. Kerminen (2003), Condensational growth of atmospheric nuclei by organic vapours, *J. Aerosol Sci.*, 34, 41–61.

Birmili, W., H. Berresheim, C. Plass-Dülmer, T. Elste, S. Gilge, A. Wiedensohler, and U. Uhrner (2003), The Hohenpeiseenberg aerosol formation experiment (HAFEX): A long-term study including size-resolved aerosol, H_2SO_4, OH, and monoterpenes measurements, *Atmos. Chem. Phys.*, 3, 361–376.

Bolsaitis, P., and J. F. Elliott (1990), Thermodynamic activities and equilibrium partial pressures for aqueous sulfuric acid solutions, *J. Chem. Eng. Data*, 35, 69–85.

Brook, J. R., L. Zhang, L. Yifan, and D. Johnson (1999), Description and evaluation of a model of deposition velocities for routine estimates of dry deposition over North America. part II: Review of past measurements and model results, *Atmos. Environ.*, 33, 5053–5070.

Cabada, J. C., S. N. Pandis, and A. L. Robinson (2002), Sources of atmospheric carbonaceous particulate matter in Pittsburgh, Pennsylvania, *J. Air Waste Manage. Assoc.*, 52(6), 732–741.

Capaldo, K. P., P. Kasibhatla, and S. N. Pandis (1999), Is aerosol production within the remote marine boundary layer sufficient to maintain observed concentrations?, *J. Geophys. Res.*, 104, 3483–3500.

Coffman, D. J., and D. A. Hegg (1995), A preliminary study of the effect of ammonia on particle nucleation in the MBL, *J. Geophys. Res.*, 100, 7147–7160.

Creasey, D. J., D. E. Heard, and J. D. Lee (2002), Eastern Atlantic Spring Experiment 1997 (EASE97): 1. Measurements of OH and HO_2 concentrations at Mace Head, Ireland, *J. Geophys. Res.*, 107(D10), 4091, doi:10.1029/2001JD000892.

DeMore, W. B., et al. (1994), Chemical kinetics and photochemical data for use in stratospheric modeling, *Tech. Rep. Eval. 10*, Jet Propul. Lab., Pasadena, Calif.

Eisele, F. L., and P. H. McMurray (1997), Recent progress in understanding particle nucleation and growth, *Philos. Trans. R. Soc. London, Ser. B*, 352(1350), 191–200.

Fuchs, N. A. (1964), *The Mechanics of Aerosols*, Elsevier, New York.

Fuchs, N. A., and A. G. Sutugin (1971), *Highly Dispersed Aerosols*, Elsevier, New York.

George, L. A., T. M. Hard, and R. J. O'Brien (1999), Measurements of free radicals OH and HO_2 in Los Angeles smog, *J. Geophys. Res.*, 104(D9), 11,643–11,655.

Heard, D. E., J. D. Lee, M. J. Pilling, and N. Carslaw (2001), Measurements of OH and HO_2 in urban environments and comparison of the predictions of photochemical models, paper presented at XXVI General Assembly, Eur. Geophys. Soc., Nice, France, 25–30 March .

Hegg, D. A. (1990), Heterogeneous production of cloud condensation nuclei in the marine atmosphere, *Geophys. Res. Lett.*, 17, 2165–2168.

Hoffman, T., et al. (1997), Formation of organic aerosols from the oxidation of biogenic hydrocarbons, *J. Atmos. Sci.*, 26, 189–222.

Hoffmann, T., C. D. O'Dowd, and J. H. Seinfeld (2001), Iodine oxide homogeneous nucleation: An explanation for coastal new particle production, *Geophys. Res. Lett.*, 28, 1949–1952.

Hummelshoj, P., N. O. Jensen, and S. E. Larsen (1992), Particle dry deposition to a sea surface, in *Precipitation Scavenging and Atmosphere Surface Exchange*, edited by S. E. Schwartz and W. G. N. Slinn, p. 829–840, Taylor and Francis, Philadelphia, Pa.

Ibald-Mulli, A., H. E. Wichmann, W. Kreyling, and A. Peters (2002), Epidemiological evidence on health effects of ultrafine particles, *J. Aerosol Med.*, 15, 189–201.

Jaecker-Voirol, A., and P. Mirabel (1989), Hetermolecular nucleation in the sulfuric acid-water system, *Atmos. Environ.*, 23, 2053–2057.

Janson, R., K. Rosman, A. Karlsson, and H.-C. Hansson (2001), Biogenic emissions and gaseous precursors to forest aerosols, *Tellus, Ser. B*, 53, 423–440.

Jefferson, A., F. L. Eisele, P. J. Ziemann, R. J. Weber, J. J. Marti, and P. H. McMurry (1997), Measurements of the H_2SO_4 mass accommodation coefficient onto polydisperse aerosol, *J. Geophys. Res.*, 102, 19,021–19,028.

Kerminen, V.-M., A. Virkkula, R. Hillamo, A. S. Wexler, and M. Kulmala (2000), Secondary organics and atmospheric cloud condensation nuclei production, *J. Geophys. Res.*, 105(D7), 9255–9264.

Kerminen, V.-M., L. Pirjola, and M. Kulmala (2001), How significantly does coagulational scavenging limit atmospheric particle production?, *J. Geophys. Res.*, 106(D20), 24,119–24,125.

Khlystov, A., G. P. Wyers, and J. Slanina (1995), The steam-jet aerosol collector, *Atmos. Environ.*, 29, 2229–2234.

Korhonen, H., K. E. J. Lehtinen, L. Pirjola, I. Napari, H. Vehkamäki, M. Noppel, and M. Kulmala (2003), Simulation of atmospheric nucleation mode: A comparison of nucleation models and size distribution representations, *J. Geophys. Res.*, 108(D15), 4471, doi:10.1029/2002JD003305.

Kreidenweis, S. M., F. Yin, S. C. Wang, D. Grosjean, R. C. Flagan, and J. H. Seinfeld (1991), Aerosol formation during photooxidation of organosulfur species, *Atmos. Environ. Part A*, 25, 2491–2500.

Kulmala, M., et al. (2001a), On the formation, growth, and composition of nuclei mode particles, *Tellus, Ser. B*, 53(4), 479–490.

Kulmala, M., L. Pirjola, and J. M. Makela (2001b), Stable sulphate clusters as a source of new atmospheric particles, *Nature*, 404(6773), 66–69.

Kulmala, M., P. Korhonen, I. Napari, A. Karlsson, H. Berresheim, and C. D. O'Dowd (2002), Aerosol formation during PARFORCE: Ternary nucleation of H_2SO_4, NH_3, and H_2O, *J. Geophys. Res.*, 107(D19), 8111, doi:10.1029/2001JD000900.

Laakso, L., J. M. Mäkelä, L. Pirjola, and M. Kulmala (2002), Model studies on ion-induced nucleation in the atmosphere, *J. Geophys. Res.*, 107(D20), 4427, doi:10.1029/2002JD002140.

Li, X. Y., D. Brown, S. Smith, W. MacNee, and K. Donaldson (1999), Short-term inflammatory responses following intratracheal instillation of fine and ultrafine carbon black in rats, *Inhal. Toxicol.*, 11, 709–731.

Mauldin, R. L., III, et al. (2001), Measurements of OH aboard the NASA P-3 during PEM-Tropics B, *J. Geophys. Res.*, 106(D23), 32,657–32,666.

Napari, I., M. Noppel, H. Vehkamäki, and M. Kulmala (2002), Parametrization of ternary nucleation rates for H_2SO_4-NH_3-H_2O vapors, *J. Geophys. Res.*, 107(D19), 4381, doi:10.1029/2002JD002132.

Nemmar, A., et al. (2002), Passage of inhaled particles into the blood circulation in humans, *Circulation*, 105(4), 411–414.

Nilsson, E. D., and M. Kulmala (1998), The potential for atmospheric mixing processes to enhance the binary nucleation rate, *J. Geophys. Res.*, 103(D1), 1381–1389.

Nilsson, E. D., U. Rannik, M. Kulmala, G. Buzorius, and C. D. O'Dowd (2001), Effects of continental boundary layer evolution, convection, turbulence and entrainment, on aerosol formation, *Tellus, Ser. B*, 53(4), 441–461.

Oberdorster, G., J. Ferin, R. Gelein, S. C. Soderholm, and J. Finkelstein (1992), Role of the alveolar macrophage in lung injury—Studies with ultrafine particles, *Environ. Health Perspect.*, 97, 193–199.

Oberdorster, G., et al. (2002), Extrapulmonary translocation of ultrafine carbon particles following whole-body inhalation exposure of rats, *J. Toxicol. Environ. Health A*, 65(20), 1531–1543.

O'Dowd, C. D., et al. (2002), A dedicated study of New Particle Formation and Fate in the Coastal Environment (PARFORCE): Overview of objectives and achievements, *J. Geophys. Res.*, 107(D19), 8108, doi:10.1029/2001JD000555.

Peters, A., H. E. Wichmann, T. Tuch, J. Heinrich, and J. Heyder (1997), Respiratory effects are associated with the number of ultrafine particles, *Am. J. Respir. Critical Care Med.*, 155(4), 1376–1383.

Pirjola, L., and M. Kulmala (2001), Development of particle size and composition distributions with a novel aerosol dynamics model, *Tellus, Ser. B*, 53(4), 491–509.

Pirjola, L., et al. (1999), Formation of sulphuric acid aerosols and cloud condensation nuclei: An expression for significant nucleation and model comparison, *J. Aerosol Sci.*, 30, 1079–1094.

Raes, F., A. Saltelli, and R. V. Dingenen (1992), Modelling formation and growth of H_2SO_4–H_2O aerosols: Uncertainty analysis and experimental evaluation, *J. Aerosol Sci.*, 23, 759–771.

Ren, X. R., et al. (2003a), HO_x concentrations and OH reactivity observations in New York City during PMTACS-NY2001, *Atmos. Environ.*, 37, 3627–3637.

Ren, X. R., et al. (2003b), OH and HO_2 Chemistry in the urban atmosphere of New York City, *Atmos. Environ.*, 37, 3639–3651.

Samet, J. M., F. Dominici, F. C. Curriero, I. Coursac, and S. L. Zeger (2000), Fine particulate air pollution and mortality in 20 U.S. cities, 1987–1994, *N. Engl. J. Med.*, 343, 1742–1749.

Seinfeld, J. H., and S. N. Pandis (1998), *Atmospheric Chemistry and Physics From Air Pollution to Climate Change*, John Wiley, Hoboken, N. J.

Stanier, C. O., A. Khylstov, and S. N. Pandis (2004a), Ambient aerosol size distributions and number concentrations measured during the Pittsburgh Air Quality Study (PAQS), *Atmos. Environ.*, 38, 3275–3284.

Stanier, C., A. Khlystov, and S. N. Pandis (2004b), Nucleation events during the Pittsburgh Air Quality Study: Description and relation to key meteorological, gas phase, and aerosol parameters, *Aerosol Sci. Technol.*, 38, suppl. 1, 253–264.

Tan, D., et al. (2001), HO_x budgets in a deciduous forest: Results from the PROPHET summer 1998 campaign, *J. Geophys. Res.*, 106(D20), 24,407–24,427.

U.S. Congress (2003), Clear Skies Act, S. 485, 108th Congress, 27 Feb.

U.S. Environmental Protection Agency (1996), Air quality criteria for particulate matter, *Rep. EPA/600/P-95/-1aF-cF.v3*, Natl. Cent. for Environ. Assess., Research Triangle Park, N. C.

Vehkamäki, H., M. Kulmala, I. Napari, K. E. J. Lehtinen, C. Timmreck, M. Noppel, and A. Laaksonen (2002), An improved parameterization for sulfuric acid-water nucleation rates for tropospheric and stratospheric conditions, *J. Geophys. Res.*, 107(D22), 4622, doi:10.1029/2002JD002184.

Weber, R. J., et al. (1996), Measured atmospheric new particle formation rates: Implications for nucleation mechanisms, *Chem. Eng. Commun.*, 151, 53–64.

Weber, R. J., et al. (1998), A study of new particle formation and growth involving biogenic and trace gas species measured during ACE 1, *J. Geophys. Res.*, 103, 16,385–16,396.

Weber, R. J., et al. (1999), New particle formation in the remote troposphere: A comparison of observations at various sites, *Geophys. Res. Lett.*, 26, 307–310.

Wexler, A. S., F. W. Lurmann, and J. H. Seinfeld (1994), Modelling urban and regional aerosols—I. Model development, *Atmos. Environ.*, 28(3), 531–546.

Wittig, B., N. Anderson, A. Y. Khlystov, S. N. Pandis, C. Davidson, and A. L. Robinson (2004), Pittsburgh Air Quality Study overview, *Atmos. Environ.*, 38, 3107–3125.

Woo, K. S., D. R. Chen, D. Y. H. Pui, and P. H. McMurry (2001), Measurement of Atlanta aerosol size distributions: Observations of ultrafine particle events, *Aerosol Sci. Technol.*, 34, 75–87.

Zhang, K. M., and A. S. Wexler (2002), A hypothesis for growth of fresh atmospheric nuclei, *J. Geophys. Res.*, 107(D21), 4577, doi:10.1029/2002JD002180.

Zhang, Q., C. Stanier, M. Caragaratna, J. T. Jayne, D. Worsnop, S. N. Pandis, and J. L. Jimenez (2004), Insights into the chemistry of nucleation bursts and particle growth events in Pittsburgh based on aerosol mass spectrometry, *Environ. Sci. Technol.*, 38, 4797–4809.

————————————

T. M. Gaydos, S. N. Pandis, and C. O. Stanier, Department of Chemical Engineering, Carnegie Mellon University, Pittsburgh, PA 15213, USA. (spyros@andrew.cmu.edu)